AIAA JOURNAL
Vol. 32, No. 3, March 1994

Buckling of Moderately Thick, Laminated Cylindrical Shells Under Torsion

A. Tabiei* and G. J. Simitses†
University of Cincinnati, Cincinnati, Ohio 45221

The problem of instability of laminated, circular cylindrical shells under the action of torsional loads is investigated. The analysis is based on higher order shear deformation theory where the effect of transverse shear is taken under consideration. The buckling is elastic for moderately thick composite shells, and the geometry is assumed to be free of initial geometric imperfections. The equilibrium equations and the related boundary conditions were derived by variational methods and the buckling equations through the perturbation technique. Three theories (higher order, first order, and classical) are compared to determine their range of applicability in predicting critical conditions for moderately thick, torsionally loaded, cylindrical shells. The effects on the buckling load of stacking sequence, radius-to-thickness ratios, and length-to-radius ratios is assessed. The numerical results are presented, for a typical graphite/epoxy material, in tabular and graphical forms.

Nomenclature

h	= thickness
L	= length
$N_{ij}, M_{ij}, K_{ij}, L_{ij}, \bar{Q}_{ij}, P_{\theta\theta}$	= integrals of stresses
$\bar{N}_{x\theta}$	= applied torsional load
$Q_{ij}, \bar{Q}_{ij}$	= lamina stiffness elements
R	= radius
u, v, w	= displacements
$\bar{u}, \bar{v}, \bar{w}$	= midsurface displacements
x, y (or θ), z	= coordinate system
δ_1	= parameter equal to zero or one
ϵ_{ij}	= strain tensor
σ_{ij}	= stress tensor
$\Psi_x, \Psi_y, \xi_x, \xi_y, \zeta_x, \zeta_y$	= parameters due to higher order expansion

Superscripts

a	= small additional parameters
p	= primary state parameters

I. Introduction

MOST of the present-day advanced composites have a low transverse shear modulus, and therefore transverse shear deformation plays a more important role in the kinematics of laminated shells than in metallic ones. The high ratios of Young's modulus to shear modulus may render classical theories inadequate for the analysis of moderately thick composite shells. The importance of transverse shear deformation in the buckling behavior of moderately thick laminated structural elements is well documented by Reddy,[1,2] Noor and Burton,[3,4] Khdeir et al.,[5] and most recently by Simitses and Anastasiadis.[6,7] The problem of torsional instability has been treated by many investigators over the years. Several efforts can be found in the literature concerning this problem. Simitses[8,9] treated the problem of buckling of eccentrically stiffened cylinders under torsion using Donnell-Batdorf-type relations. More recently Simitses and Han[10] analyzed the buckling of laminated cylindrical shells subjected to torsion using classical, Sanders-type shell theory. No efforts are reported for the study of the buckling of shells under the action of torsion based on shear deformable shell theory.

Few results concerning critical loads are being generated by employing shear deformation shell theories. Therefore, it is important to identify the structural parameters (stiffnesses, geometry, etc.) which influence the requirement of use of shear deformation theories for accurate prediction of buckling loads. Furthermore, it is important to establish the parameter range over which the various shell theories (classical, first order, and higher order) yield predictions (of critical loads) of acceptable magnitudes. Extensive parametric studies are performed and various stacking sequences are considered to establish preferred fiber orientations without applying a formal optimization technique.

The present work deals with the development of the kinematic relations, equilibrium equations and related boundary conditions, and buckling equations and related boundary conditions, for a laminated, cylindrical, moderately thick shell, including the effect of transverse shear. A higher order displacement field in the thickness direction is employed. Finally, buckling applications are presented for moderately thick, torsionally loaded, laminated cylindrical shells with fixed ends. The results are compared to the critical loads obtained using first order shear deformation theory and classical theory.

II. Mathematical Formulation

The cylindrical shell is assumed to be relatively thick, geometrically perfect, and have a laminated construction which is symmetric with respect to the midsurface. The material behavior is linearly elastic, the laminas are orthotropic, and the loading is torsional.

A. Kinematic Relations

1. Higher Order Shear Deformation Theory

From the exact nonlinear theory of elasticity for strains, and by performing a power series expansion and retaining terms to the second degree, the following expressions for the strains are obtained (for details see Ref. 11):

$$\epsilon_{xx} = u_{,x} + \tfrac{1}{2}v_{,x}^2 + \tfrac{1}{2}w_{,x}^2$$

Received Dec. 28, 1992; presented as Paper 93-1334 at the AIAA/ASME/ASCE/AHS/ASC 34th Structures, Structural Dynamics, and Materials Conference, La Jolla, CA, April 19-21, 1993; revision received May 1, 1993; accepted for publication May 5, 1993.

*Graduate Research Assistant, Department of Aerospace Engineering and Engineering Mechanics. Student Member AIAA.

†Professor and Head, Department of Aerospace Engineering and Engineering Mechanics. Associate Fellow AIAA.

$$\epsilon_{\theta\theta} = \frac{w}{(R+z)} + \frac{v_{,\theta}}{(R+z)} + \frac{1}{2}\left[\frac{w_{,\theta}}{(R+z)} + \frac{v}{(R+z)}\right]^2 + \frac{1}{2}\frac{u_{,\theta}^2}{(R+z)^2}$$

$$\epsilon_{zz} = w_{,x} + \tfrac{1}{2}u_{,z}^2 + \tfrac{1}{2}v_{,z}^2$$

$$\gamma_{x\theta} = \frac{u_{,\theta}}{(R+z)}\left[1 - \frac{v_{,\theta}}{(R+z)} - \frac{w}{(R+z)}\right] + v_{,x}(1-u_{,x}) + w_{,x}\left[\frac{w_{,\theta}}{(R+z)} - \frac{v}{(R+z)}\right]$$

$$\gamma_{xz} = w_{,x}(1-u_{,x}) + u_{,z}(1-w_{,z}) + v_{,x}v_{,z}$$

$$\gamma_{\theta z} = v_{,z}(1-w_{,z}) + \left[\frac{w_{,\theta}}{(R+z)} - \frac{v}{(R+z)}\right]\times\left[1 - \frac{v_{,\theta}}{(R+z)} - \frac{w}{(R+z)}\right] + \frac{u_{,\theta}u_{,z}}{(R+z)} \tag{1}$$

A general cubic variation in the z coordinate is assumed for u (axial displacement) and v (circumferential displacement), whereas w (along the thickness displacement) is independent of z.

$$u(x,y,z) = \bar{u}(x,y) + z\Psi_x(x,y) + z^2\xi_x(x,y) + z^3\zeta_x(x,y)$$

$$v(x,y,z) = \bar{v}(x,y) + z\Psi_y(x,y) + z^2\xi_y(x,y) + z^3\zeta_y(x,y)$$

$$w(x,y,z) = \bar{w}(x,y) \tag{2}$$

where $\bar{u}(x,y)$, $\bar{v}(x,y)$, and $\bar{w}(x,y)$ are reference surface displacements; and Ψ_x, ξ_x, ζ_x, Ψ_y, ξ_y, ζ_y are functions of position on the reference surface (x,y). For the purpose of this work, concentration to problems where the rotations [$\bar{w}_{,x}$ and $\bar{w}_{,y} - (\delta_1\bar{v}/R+z)$] are moderately small is made.[11] Note that if $\delta_1 = 0$ then Donnell-type relations are obtained. Thus, products containing these terms are retained and the remaining products are neglected as small by comparison. Substitution of the displacement relations into the strain expressions, and the knowledge of zero shear tractions on the upper and lower surfaces, lead to the final kinematic relations, which can be written in the following form:

$$\epsilon_{xx} = \epsilon_{xx}^o + zK_{xx}^1 + z^3K_{xx}^3$$

$$\epsilon_{\theta\theta} = \frac{1}{(R+z)^2}K_{\theta\theta}^{-2} + \frac{1}{(R+z)}K_{\theta\theta}^{-1} + \epsilon_{\theta\theta}^o + zK_{\theta\theta}^1 + z^2K_{\theta\theta}^2$$

$$\epsilon_{zz} = 0$$

$$\gamma_{x\theta} = \frac{1}{(R+z)}K_{x\theta}^{-1} + \gamma_{x\theta}^o + zK_{x\theta}^1 + z^2K_{x\theta}^2 + z^3K_{x\theta}^3$$

$$\gamma_{xx} = \gamma_{xz}^o + z^2K_{xz}^2$$

$$\gamma_{z\theta} = \frac{1}{(R+z)}K_{z\theta}^{-1} + \gamma_{z\theta}^o + zK_{z\theta}^1 + z^2K_{z\theta}^2 \tag{3}$$

where

$$\epsilon_{xx}^o = \bar{u}_{,x} + \tfrac{1}{2}\bar{w}_{,x}^2 \qquad K_{xx}^1 = \Psi_{x,x}$$

$$K_{xx}^3 = -\frac{4}{3h^2}(\bar{w}_{,xx} + \Psi_{x,x}) \qquad K_{\theta\theta}^{-2} = \tfrac{1}{2}(\bar{w}_{,\theta} - \delta_1\bar{v})^2$$

$$K_{\theta\theta}^{-1} = \bar{w} + \bar{v}_{,\theta} - R\Psi_{y,\theta} + \frac{R^3(\Delta_1-\Delta_3)}{\Delta_1}\left(\Psi_{y,\theta} + \frac{\bar{w}_{,\theta\theta}}{R} - \delta_1\frac{\bar{v}_{,\theta}}{R}\right)$$

$$\epsilon_{\theta\theta}^o = \Psi_{y,\theta} + \frac{R^2(\Delta_1-\Delta_3)}{\Delta_1}\left(\Psi_{y,\theta} + \frac{\bar{w}_{,\theta\theta}}{R} - \delta_1\frac{\bar{v}_{,\theta}}{R}\right)$$

$$K_{\theta\theta}^1 = \frac{R(\Delta_1-\Delta_3)}{\Delta_1}\left(\Psi_{y,\theta} + \frac{\bar{w}_{,\theta\theta}}{R} - \delta_1\frac{\bar{v}_{,\theta}}{R}\right)$$

$$K_{\theta\theta}^2 = \frac{\Delta_3}{\Delta_1}\left(\Psi_{y,\theta} + \frac{\bar{w}_{,\theta\theta}}{R} - \delta_1\frac{\bar{v}_{,\theta}}{R}\right)$$

$$K_{x\theta}^{-1} = \bar{u}_{,\theta} - R\Psi_{x,\theta} + \frac{4R^3}{3h^2}(\bar{w}_{,x\theta} + \Psi_{x,\theta}) + \bar{w}_{,x}\bar{w}_{,\theta} - \delta_1\overline{vw}_{,x}$$

$$\gamma_{x\theta}^o = \Psi_{x,\theta} - \frac{4R^2}{3h^2}(\bar{w}_{,x\theta} + \Psi_{x,\theta}) + \bar{v}_{,x}$$

$$K_{x\theta}^1 = \frac{4R}{3h^2}(\bar{w}_{,x\theta} + \Psi_{x,\theta}) + \Psi_{y,x}$$

$$K_{x\theta}^2 = -\frac{4}{3h^2}(\bar{w}_{,x\theta} + \Psi_{x,\theta}) + \frac{R\Delta_2}{\Delta_1}\left(\Psi_{y,x} + \frac{\bar{w}_{,x\theta}}{R} - \delta_1\frac{\bar{v}_{,x}}{R}\right)$$

$$K_{x\theta}^3 = \frac{\Delta_3}{\Delta_1}\left(\Psi_{y,x} + \frac{\bar{w}_{,x\theta}}{R} - \delta_1\frac{\bar{v}_{,x}}{R}\right)$$

$$\gamma_{xz}^o = \bar{w}_{,x} + \Psi_x$$

$$K_{xz}^2 = -\frac{4}{h^2}(\bar{w}_{,x} + \Psi_x)$$

$$K_{z\theta}^{-1} = -\frac{R^3(\Delta_2-\Delta_3)}{\Delta_1}\left(\Psi_y + \frac{\bar{w}_{,\theta}}{R} - \delta_1\frac{\bar{v}}{R}\right) + \bar{w}_{,\theta} + R\Psi_y - \delta_1\bar{v}$$

$$\gamma_{z\theta}^o = \frac{R^2(\Delta_2-\Delta_3)}{\Delta_1}\left(\Psi_y + \frac{\bar{w}_{,\theta}}{R} - \delta_1\frac{\bar{v}}{R}\right)$$

$$K_{z\theta}^1 = \frac{R(\Delta_2+\Delta_3)}{\Delta_1}\left(\Psi_y + \frac{\bar{w}_{,\theta}}{R} - \delta_1\frac{\bar{v}}{R}\right)$$

$$K_{z\theta}^2 = \frac{2\Delta_3}{\Delta_1}\left(\Psi_y + \frac{\bar{w}_{,\theta}}{R} - \delta_1\frac{\bar{v}}{R}\right)$$

$$\Delta_1 = h^2(16h^2R^2 - 48R^4 - h^4)$$

$$\Delta_2 = 4h^2(h^2 - 4R^2)$$

$$\Delta_3 = 16R^2(4R^2 - h^2)$$

2. First-Order Shear Deformation Theory

The kinematic relations corresponding to the first-order shear deformation theory can be concluded from the kinematic relations for the higher order shear deformation theory by assuming that γ_{xz} and $\gamma_{\theta z}$ are independent of z (along the thickness coordinate). The final kinematic relations for the first-order shear deformation theory can be written in the following form (for details see Ref. 7):

$$\epsilon_{xx} = \epsilon_{xx}^o + zK_{xx}^1 \qquad \epsilon_{\theta\theta} = \frac{1}{(R+z)^2}K_{\theta\theta}^{-2} + \frac{1}{(R+z)}K_{\theta\theta}^{-1} + \epsilon_{\theta\theta}^o$$

$$\epsilon_{zz} = 0 \qquad \gamma_{x\theta} = \frac{1}{(R+z)}K_{x\theta}^{-1} + \gamma_{x\theta}^o + zK_{x\theta}^1$$

$$\gamma_{xz} = \gamma_{xz}^o \qquad \gamma_{z\theta} = \frac{1}{(R+z)}K_{z\theta}^{-1}$$

where

$$\epsilon_{xx}^o = \bar{u}_{,x} + \tfrac{1}{2}\bar{w}_{,x}^2 \qquad K_{xx}^1 = \Psi_{x,x} \qquad K_{\theta\theta}^{-2} = \tfrac{1}{2}(\bar{w}_{,\theta} - \delta_1\bar{v})^2$$

$$K_{\theta\theta}^{-1} = \bar{w} + \bar{v}_{,\theta} - R\Psi_{y,\theta} \qquad \epsilon_{\theta\theta}^o = \Psi_{y,\theta}$$

$$K_{x\theta}^{-1} = \bar{u}_{,\theta} - R\Psi_{x,\theta} + \bar{w}_{,x}\bar{w}_{,\theta} - \delta_1\overline{vw}_{,x}$$

$$\gamma_{x\theta}^o = \Psi_{x,\theta} + \bar{v}_{,x} \qquad K_{x\theta}^1 = \Psi_{y,x} \qquad \gamma_{xz}^o = \bar{w}_{,x} + \Psi_x$$

$$K_{z\theta}^{-1} = \bar{w}_{,\theta} + R\Psi_y - \delta_1\bar{v}$$

3. Classical Theory

The kinematic relations corresponding to the classical theory can be concluded from the kinematic relations for the first-order shear deformation theory by setting $\gamma_{xz}=\gamma_{\theta z}=0$. The final kinematic relations for the classical theory can be written in the following form:

$$\epsilon_{xx}=\epsilon^o_{xx}+zK^1_{xx} \qquad \epsilon_{\theta\theta}=\epsilon^o_{\theta\theta}+\frac{1}{(R+z)}K^1_{\theta\theta}$$

$$\gamma_{x\theta}=\gamma^o_{x\theta}+zK^1_{x\theta} \qquad \epsilon_{zz}=\gamma_{\theta z}=\gamma_{xz}=0$$

where

$$\epsilon^o_{xx}=\bar{u}_{,x}+\tfrac{1}{2}\bar{w}^2_{,x} \qquad \epsilon^o_{\theta\theta}=\frac{1}{R}(\bar{w}+\bar{v}_{,\theta})+\frac{1}{2R^2}(\bar{w}_{,\theta}-\delta_1\bar{v})^2$$

$$\gamma^o_{x\theta}=\bar{v}_{,x}+\frac{\bar{u}_{,\theta}}{R}+\frac{1}{R}\bar{w}_{,x}(\bar{w}_{,\theta}-\delta_1\bar{v}) \qquad K^1_{xx}=-\bar{w}_{,xx}$$

$$K^1_{\theta\theta}=-\frac{1}{R^2}(\bar{w}_{\theta\theta}-\delta_1\bar{v}_{,\theta}) \qquad K^1_{x\theta}=-\frac{1}{R}(2\bar{w}_{,x\theta}-\delta_1\bar{v}_{,x})$$

B. Constitutive Relations

The equations relating the stresses to the strains for a laminate, in terms of structural axes coordinates, are given by (for details see Ref. 14):

$$\begin{Bmatrix}\sigma_{xx}\\ \sigma_{\theta\theta}\\ \sigma_{zz}\\ \sigma_{z\theta}\\ \sigma_{xz}\\ \sigma_{x\theta}\end{Bmatrix}=\begin{bmatrix}\bar{Q}_{11}&\bar{Q}_{12}&\bar{Q}_{13}&0&0&\bar{Q}_{16}\\ \bar{Q}_{12}&\bar{Q}_{22}&\bar{Q}_{23}&0&0&\bar{Q}_{26}\\ \bar{Q}_{13}&\bar{Q}_{23}&\bar{Q}_{33}&0&0&\bar{Q}_{36}\\ 0&0&0&\bar{Q}_{44}&\bar{Q}_{45}&0\\ 0&0&0&\bar{Q}_{45}&\bar{Q}_{55}&0\\ \bar{Q}_{16}&\bar{Q}_{26}&\bar{Q}_{36}&0&0&\bar{Q}_{66}\end{bmatrix}\begin{Bmatrix}\epsilon_{xx}\\ \epsilon_{\theta\theta}\\ \epsilon_{zz}\\ \gamma_{z\theta}\\ \gamma_{xz}\\ \gamma_{x\theta}\end{Bmatrix} \tag{4}$$

where the $\bar{Q}_{ij}$ are given in terms of the orthotropic stiffnesses Q_{ij}, through the usual transformation equations.

C. Governing Equations

Use of the principle of the stationary value of the total potential energy yields the equilibrium equations and associated boundary conditions. The kinematic relations used to obtain the equilibrium equations for the three theories are of Donnell type (setting $\delta_1=0$). Only the equilibrium equations corresponding to the higher order theory are shown herein:

$$RN_{xx,x}+M_{xx,x}+N_{x\theta,\theta}=0$$

$$N_{\theta\theta,\theta}+RN_{x\theta,\theta}+M_{x\theta,\theta}=0$$

$$\frac{\Delta_2}{\Delta_1}K_{\theta\theta,\theta\theta}-\frac{4}{3h^2}\tilde{Q}_{xx,xx}-R(N_{xx}\bar{w}_{,x})_{,x}-(M_{xx}\bar{w}_{,x})_{,x}$$
$$+N_{\theta\theta}-\frac{4R}{3h^2}L_{xx,xx}+\frac{\Delta_3}{R\Delta_1}L_{\theta\theta,\theta\theta}$$
$$-(P_{\theta\theta}\bar{w}_{,\theta})_{,\theta}+\frac{R\Delta_2}{\Delta_1}K_{x\theta,x\theta}+\left(\frac{\Delta_2+\Delta_3}{\Delta_1}-\frac{4}{3h^2}\right)L_{x\theta,x\theta}$$
$$+\frac{\Delta_3}{R\Delta_1}\tilde{Q}_{x\theta,x\theta}-(N_{x\theta}\bar{w}_{,\theta})_{,x}-(N_{x\theta}\bar{w}_{,x})_{,\theta}-RN_{xz,x}$$
$$-M_{xz,x}+\frac{4R}{h^2}K_{xz,x}+\frac{4}{h^2}L_{xz,x}-N_{\theta z,\theta}-\frac{2R\Delta_2}{\Delta_1}M_{\theta z,\theta}$$
$$-\frac{\Delta_2+3\Delta_3}{\Delta_1}K_{\theta z,\theta}-\frac{2\Delta_3}{R\Delta_1}L_{\theta z,\theta}=0$$

$$\frac{4R}{3h^2}L_{xx,x}-RM_{xx,x}-K_{xx,x}+\frac{4}{3h^2}\tilde{Q}_{xx,x}-M_{x\theta,\theta}$$
$$+\frac{4}{3h^2}L_{x\theta,\theta}+RN_{xz}-\frac{4R}{h^2}K_{xz}+M_{xz}-\frac{4}{h^2}L_{xz}=0$$

$$RN_{\theta z}-\frac{R\Delta_2}{\Delta_1}K_{\theta\theta,\theta}-\frac{\Delta_3}{\Delta_1}L_{\theta\theta,\theta}-RM_{x\theta,x}-\left(1+\frac{R^2\Delta_2}{\Delta_1}\right)K_{x\theta,x}$$
$$-\frac{R(\Delta_2+\Delta_3)}{\Delta_1}L_{x\theta,x}-\frac{\Delta_3}{\Delta_1}\tilde{Q}_{x\theta,x}-M_{\theta\theta,\theta}+\frac{2R^2\Delta_2}{\Delta_1}M_{\theta z}$$
$$+\frac{R(\Delta_2+\Delta_3)}{\Delta_1}K_{\theta z}+\frac{2\Delta_3}{\Delta_1}L_{\theta z}=0 \tag{5}$$

with the following boundary conditions at $x=0, L$

Either	Or
$RN_{xx}+M_{xx}=0$	$\delta\bar{u}=0$
$RN_{x\theta}+M_{x\theta}=-R\bar{N}_{x\theta}$	$\delta\bar{v}=0$
$\frac{4R}{3h^2}L_{xx,x}-\frac{4}{3h^2}\tilde{Q}_{xx,x}-RN_{xx}\bar{w}_{,x}+M_{xx}\bar{w}_{,x}$ $-\frac{R\Delta_2}{\Delta_1}K_{x\theta,\theta}-\frac{\Delta_3}{R\Delta_1}(\tilde{Q}_{x\theta,x}+\tilde{Q}_{x\theta,\theta})+N_{x\theta}\bar{w}_{,\theta}$ $+RN_{xz}+M_{xz}-\frac{4}{h^2}K_{xz}-\frac{4}{h^2}L_{xz}-\frac{R\Delta_2}{\Delta_1}K_{x\theta,x}$ $-\left(\frac{\Delta_2+\Delta_3}{\Delta_1}-\frac{4}{3h^2}\right)(L_{x\theta,x}+L_{x\theta,\theta})=0$	$\delta\bar{w}=0$
$RM_{xx}-\frac{4R}{3h^2}L_{xx}+K_{xx}-\frac{4}{3h^2}\tilde{Q}_{xx}=0$	$\delta\Psi_x=0$
$RM_{x\theta}+\left(1+\frac{R^2\Delta_2}{\Delta_1}\right)K_{x\theta}+\frac{R(\Delta_2+\Delta_3)}{\Delta_1}L_{x\theta}$ $+\frac{\Delta_3}{\Delta_1}\tilde{Q}_{x\theta}=0$	$\delta\Psi_y=0$
$\frac{4R}{3h^2}L_{xx}+\frac{4}{3h^2}\tilde{Q}_{xx}=0$	$\delta\bar{w}_{,x}=0$

where

$$N_{ij},M_{ij},K_{ij},L_{ij},\tilde{Q}_{ij}=\int_{-(h/2)}^{h/2}\sigma_{ij}(1,z,z^2,z^3,z^4)\,dz$$

$$P_{\theta\theta}=\int_{-(h/2)}^{h/2}\frac{\sigma_{ij}}{R+z}\,dz \tag{6}$$

D. Buckling Equations

1. Prebuckling State

The shell is free of initial geometric imperfections, the laminate is symmetric with respect to the midsurface, and the only loading is torsion. These conditions allow the existence of a prebuckling state, and bifurcation buckling is possible. The primary state solution is found to be the following:

$$\bar{u}^p=Ax$$

$$\bar{v}^p=Bx+C\theta$$

$$\bar{w}^p=\Psi^p_x=\Psi^p_y=0 \tag{7}$$

where the constants A, B, and C are found in terms of the applied load $\bar{N}_{x\theta}$ and the shell stiffness parameters (defined in the Appendix). The preceding solution is applicable to the three theories considered.

2. Buckling State

Once the prebuckling state solution is known, the perturbation technique[12] can be applied to produce the buckling equations and the related boundary conditions. The buckling equations can be derived by assuming that we can pass from the primary to the buckled state through extremely small additional parameters so that linearization is possible. Let $(\ )^p$ denote the primary state parameters and $(\ )^a$ denote the small additional parameters needed to take us from the primary state to an adjacent buckled state. Then, by allowing small admissible variation in $\bar{u}$, $\bar{v}$, $\bar{w}$, Ψ_x, and Ψ_y one obtains:

$$N_{ij} = (N_{ij})^a + (N_{ij})^p, \qquad M_{ij} = (M_{ij})^a + (N_{ij})^p$$
$$K_{ij} = (K_{ij})^a + (K_{ij})^p, \qquad L_{ij} = (L_{ij})^a + (L_{ij})^p$$
$$\tilde{Q}_{ij} = (\tilde{Q}_{ij})^a + (\tilde{Q}_{ij})^p, \qquad P_{ij} = (P_{ij})^a + (P_{ij})^p \tag{8}$$

Expressing the given primary state quantities in terms of the displacements and using the prebuckling solution leads to

$$(N_{x\theta})^p = A_{16}\cdot A + A_{66}\cdot B + T_{26}\cdot C = -\bar{N}_{x\theta}$$
$$(M_{xx})^p = AA_{12}\cdot C$$
$$(M_{\theta\theta})^p = AA_{22}\cdot C$$
$$(M_{x\theta})^p = AA_{26}\cdot C$$
$$(P_{\theta\theta})^p = T_{12}\cdot A + T_{26}\cdot B + R_{22}\cdot C \tag{9}$$

and all of the other primary state quantities are zero. The final buckling equations and corresponding boundary conditions, after dropping the superscript a, are as follows:

$$RN_{xx,x} + M_{xx,x} + N_{x\theta,\theta} = 0$$
$$N_{\theta\theta,\theta} + RN_{x\theta,\theta} + M_{x\theta,\theta} = 0$$
$$\frac{\Delta_2}{\Delta_1}K_{\theta\theta,\theta\theta} - \frac{4}{3h^2}\tilde{Q}_{xx,xx} - (M_{xx})^p\bar{w}_{,xx} + N_{\theta\theta} - \frac{4R}{3h^2}L_{xx,xx}$$
$$+ \frac{\Delta_3}{R\Delta_1}L_{\theta\theta,\theta\theta} - (P_{\theta\theta})^p\bar{w}_{,\theta\theta} + \frac{R\Delta_2}{\Delta_1}K_{x\theta,x\theta}$$
$$+ \left(\frac{\Delta_2+\Delta_3}{\Delta_1} - \frac{4}{3h^2}\right)L_{x\theta,x\theta} + \frac{\Delta_3}{R\Delta_1}\tilde{Q}_{x\theta,x\theta} - 2\bar{N}_{x\theta}\bar{w}_{,x\theta}$$
$$- RN_{xz,x} - M_{xz,x} + \frac{4R}{h^2}K_{xz,x} + \frac{4}{h^2}L_{xz,x} - N_{\theta z,\theta}$$
$$- \frac{2R\Delta_2}{\Delta_1}M_{\theta z,\theta} - \frac{\Delta_2+3\Delta_3}{\Delta_1}K_{\theta z,\theta} - \frac{2\Delta_3}{R\Delta_1}L_{\theta z,\theta} = 0$$
$$\frac{4R}{3h^2}L_{xx,x} - RM_{xx,x} - K_{xx,x} + \frac{4}{3h^2}\tilde{Q}_{xx,x} - M_{x\theta,\theta} + \frac{4}{3h^2}L_{x\theta,\theta}$$
$$+ RN_{xz} - \frac{4R}{h^2}K_{xz} + M_{xz} - \frac{4}{h^2}L_{xz} = 0$$
$$RN_{\theta z} - \frac{R\Delta_2}{\Delta_1}K_{\theta\theta,\theta} - \frac{\Delta_3}{\Delta_1}L_{\theta\theta,\theta} - RM_{x\theta,x} - \left(1+\frac{R^2\Delta_2}{\Delta_1}\right)K_{x\theta,x}$$
$$- \frac{R(\Delta_2+\Delta_3)}{\Delta_1}L_{x\theta,x} - \frac{\Delta_3}{\Delta_1}\tilde{Q}_{x\theta,x} - M_{\theta\theta,\theta} + \frac{2R^2\Delta_2}{\Delta_1}M_{\theta z}$$
$$+ \frac{R(\Delta_2+\Delta_3)}{\Delta_1}K_{\theta z} + \frac{2\Delta_3}{\Delta_1}L_{\theta z} = 0 \tag{10}$$

Either	Or
$RN_{xx} + M_{xx} = 0$	$\delta\bar{u} = 0$
$RN_{x\theta} + M_{x\theta} = 0$	$\delta\bar{v} = 0$
$\frac{4R}{3h^2}L_{xx,x} - \frac{4}{3h^2}\tilde{Q}_{xx,x} - RN_{xx}\bar{w}_{,x} + M_{xx}\bar{w}_{,x} - \frac{R\Delta_2}{\Delta_1}K_{x\theta,\theta}$ $- \frac{\Delta_3}{R\Delta_1}(\tilde{Q}_{x\theta,x} + \tilde{Q}_{x\theta,\theta}) + N_{x\theta}\bar{w}_{,\theta} + RN_{xz} + M_{xz}$ $- \frac{4R}{h^2}K_{xz} - \frac{4}{h^2}L_{xz} - \frac{R\Delta_2}{\Delta_1}K_{x\theta,x}$ $- \left(\frac{\Delta_2+\Delta_3}{\Delta_1} - \frac{4}{3h^2}\right)(L_{x\theta,x} + L_{x\theta,\theta}) = 0$	$\delta\bar{w} = 0$
$RM_{xx} - \frac{4R}{3h^2}L_{xx} + K_{xx} - \frac{4}{3h^2}\tilde{Q}_{xx} = 0$	$\delta\Psi_x = 0$
$RM_{x\theta} + \left(1+\frac{R^2\Delta_2}{\Delta_1}\right)K_{x\theta} + \frac{R(\Delta_2+\Delta_3)}{\Delta_1}L_{x\theta}$ $+ \frac{\Delta_3}{\Delta_1}\tilde{Q}_{x\theta} = 0$	$\delta\Psi_y = 0$
$\frac{4R}{3h^2}L_{xx} + \frac{4}{3h^2}\tilde{Q}_{xx} = 0$	$\delta\bar{w}_{,x} = 0$

where the small additional integrated stresses are still defined by Eqs. (6) and are related to the kinematics through the relations defined in the Appendix. The buckling equations and the related boundary conditions can then be expressed in terms of the displacements $\bar{u}$, $\bar{v}$, $\bar{w}$, Ψ_x, and Ψ_y using the linearized Sanders-type kinematic relations ($\delta_1 = 1$). The justification for using Donnell-type relations for equilibirum and then Sanders-type relations for buckling is that the rotation $v/(R+z)$ is more important in the buckling state.

III. Solution Procedure and Results

A solution in the form of a double trigonometric series in the x and the y (or θ) directions is employed for all five variables $\bar{u}$, $\bar{v}$, $\bar{w}$, Ψ_x, and Ψ_y (the form of the series is given subsequently). Each term in the series satisfies the boundary conditions. The Galerkin procedure is used, and substitution into the Galerkin integrals leads to a system of linear algebraic equations in the series coefficients. For a nontrivial solution to exist the determinant of the coefficients must vanish.

$$U_i = \sum_{m=0}^{M}\sum_{n=0}^{N}\left[U_{i_{mn}}\sin(n\theta) + U'_{i_{mn}}\cos(n\theta)\right] \times \left[\cos\frac{m\pi x}{L} - \cos\frac{(m-2)\pi x}{L}\right] \tag{11}$$

where $i = 1, 2, 3, 4, 5$;

$$U_1 = \bar{u}, \qquad U_2 = \bar{v}, \qquad U_3 = \bar{w}, \qquad U_4 = \Psi_x, \qquad U_5 = \Psi_y$$

For data generation a computer program was written and numerical results were obtained by employing the Cray Y-MP machine of the Ohio Super Computer Center.

A. Geometries and Material Properties

The material considered is graphite/epoxy with the following properties:

$$E_{11} = 149.617\times10^9\ \text{Pa}, \qquad E_{22} = 9.928\times10^9\ \text{Pa}$$
$$E_{33} = 9.928\times10^9\ \text{Pa}, \qquad G_{12} = 4.481\times10^9\ \text{Pa}$$
$$G_{13} = 4.481\times10^9\ \text{Pa}, \qquad G_{23} = 2.551\times10^9\ \text{Pa}$$
$$\nu_{12} = 0.28, \qquad \nu_{13} = 0.28, \qquad \nu_{23} = 0.45$$

Nine different stacking sequences, given in degrees, are considered:

$$(0, 0, 0)_s, \quad (0, 90, 0)_s, \quad (90, 90, 0)_s$$

$$(-45, 45, -45)_s, \quad (0, 90, 90)_s, \quad (-45, -45, 45)_s$$

$$(45, -45, -45)_s, \quad (45, 45, -45)_s, \quad (30, 30, -60)_s$$

The cylinder radius is $R = 0.1905$ m and the length is varied such that $L/R = 1, 2, 5$. The total thickness values of $h = 0.001905$ m, 0.003175 m, 0.00635 m, and 0.0127 m are considered.

B. Numerical Results

Results are presented for cylinders under torsion for a graphite/epoxy material and nine stacking sequences, Moreover, several R/h ratios and L/R ratios are considered to establish the range of applicability of each shell theory. Three theories are employed in the generation of results: classical theory (CL), first-order shear deformation theory (FOSD), and higher order shear deformation theory (HOSD). Because in the FOSD theory the transverse shear strains are assumed to be constant within each layer (constant along the thickness), a correction factor has to be used to adjust the transverse shear stiffnesses and match the response predicted by the two-dimensional theory with that of the three-dimensional elasticity theory. Some results are presented for first-order shear deformation theory with a shear correction factor (FOSD-W/SCF) of 5/6. This value was kept constant for all stacking sequences and represents a modest, conservative value.

To establish a confidence factor of the developed equations (considering the fact that Donnell-type relations were employed in deriving the equilibrium equation and then Sanders-type relations were employed in the buckling equations), a comparison is made to some results from the analysis by Simitses and Han.[10] Figure 1 shows results predicted by CL for CC-4-type boundary conditions, and those of Simitses and Han[10] for SS-4-type boundary conditions, in which the typical Sanders-type analysis was employed. The results are of the usual trend: as the cylinder becomes long the values of the critical loads for the two different boundary conditions converge to each other.[13]

The results are presented in both tabular and graphical forms. Tables 1-9 show the critical torsional loads and the number of full waves for all stacking sequences considered. Each of the tables contains results for all four thicknesses and for all three theories, classical, first, and higher order shear deformation theories. For the last thickness $h = 0.0127$ m, results are also presented for the case of first-order theory with a shear correction factor equal to 5/6. Note that there is a $\pm 0.1\%$ error in the predicted values due to the step size limitation for the iteration procedure.

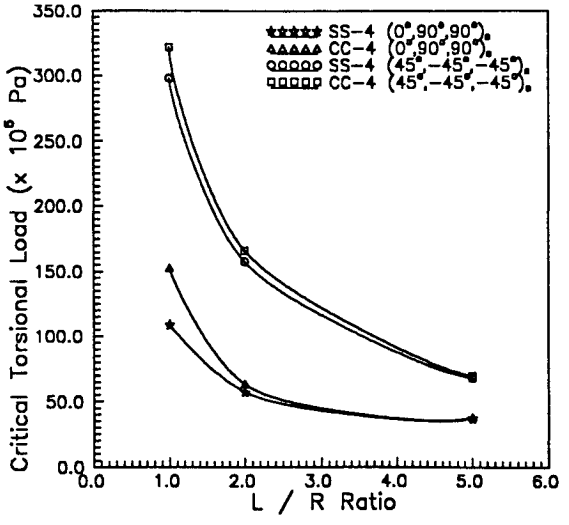

Fig. 1 Critical torsional load for CC-4- and SS-4-type boundary conditions, $R/h = 30$.

Table 1 Critical torsional load ($N/m \times 10^6$)/wave number $(0, 0, 0\ \text{deg})_s$

	$L/R = 1$	$L/R = 2$	$L/R = 5$
	$h = 0.001905$ m		
CL	0.1077/11	0.0569/10	0.0363/7
FOSD	0.1068/11	0.0567/10	0.0363/7
HOSD	0.1051/11	0.0567/10	0.0363/7
	$h = 0.003175$ m		
CL	0.4379/10	0.1839/7	0.1103/6
FOSD	0.4239/10	0.1830/7	0.1103/6
HOSD	0.4168/10	0.1822/7	0.1103/6
	$h = 0.00635$ m		
CL	3.2219/8	1.0509/6	0.5167/5
FOSD	2.7148/9	1.0228/6	0.5149/5
HOSD	2.6097/9	1.0089/6	0.5141/5
	$h = 0.0127$ m		
CL	25.206/7	6.9359/5	2.5572/4
FOSD	14.450/8	5.9026/5	2.4696/4
HOSD	13.557/8	5.6994/5	2.4556/4
FOSD-W/SCF	13.416/8	5.7379/5	2.4608/4

Table 2 Critical torsional load ($N/m \times 10^6$)/wave number $(0, 90, 0\ \text{deg})_s$

	$L/R = 1$	$L/R = 2$	$L/R = 5$
	$h = 0.001905$ m		
CL	0.1576/9	0.0989/7	0.0757/6
FOSD	0.1568/9	0.0987/7	0.0757/6
HOSD	0.1559/9	0.0987/7	0.0757/6
	$h = 0.003175$ m		
CL	0.5850/7	0.3109/7	0.2215/5
FOSD	0.5710/7	0.3100/7	0.2215/5
HOSD	0.5622/7	0.3083/7	0.2207/5
	$h = 0.00635$ m		
CL	3.8796/6	1.6114/5	0.9738/4
FOSD	3.3629/6	1.5540/5	0.9598/4
HOSD	3.2665/6	1.5326/5	0.9563/4
	$h = 0.0127$ m		
CL	29.320/5	9.2480/4	4.2910/3
FOSD	17.822/5	8.0040/4	4.1510/3
HOSD	16.499/6	7.7590/4	4.0985/3
FOSD-W/SCF	16.201/6	7.7941/4	4.1248/3

Table 3 Critical torsional load ($N/m \times 10^6$)/wave number $(0, 90, 90\ \text{deg})_s$

	$L/R = 1$	$L/R = 2$	$L/R = 5$
	$h = 0.001905$ m		
CL	0.1611/8	0.1002/7	0.0736/5
FOSD	0.1603/8	0.0998/7	0.0736/5
HOSD	0.1585/9	0.0998/7	0.0736/5
	$h = 0.003175$ m		
CL	0.5903/7	0.3170/6	0.2233/4
FOSD	0.5710/7	0.3153/6	0.2224/4
HOSD	0.5657/7	0.3135/6	0.2224/4
	$h = 0.00635$ m		
CL	3.8708/6	1.6464/5	0.9896/4
FOSD	3.3279/6	1.5939/5	0.9808/4
HOSD	3.1545/6	1.5606/5	0.9738/4
	$h = 0.0127$ m		
CL	28.602/6	9.4060/4	4.3787/3
FOSD	16.762/6	8.0390/4	4.2299/3
HOSD	15.334/6	7.7070/4	4.1826/3
FOSD-W/SCF	15.632/6	7.8292/4	4.2071/3

IV. Discussion and Conclusion

To achieve different R/h ratios, the radius is kept constant and the thickness is varied. The total thickness values of $h = 0.001905$ m, 0.003175 m, 0.00635 m, and 0.0127 m correspond to $R/h = 100$, 60, 30, and 15, respectively. The first two

Table 4 Critical torsional load ($N/m \times 10^6$)/wave number (90, 90, 0 deg)$_s$

	$L/R=1$	$L/R=2$	$L/R=5$
	$h=0.001905$ m		
CL	0.1708/8	0.1463/6	0.1249/5
FOSD	0.1690/8	0.1454/7	0.1245/5
HOSD	0.1681/8	0.1454/7	0.1244/5
	$h=0.003175$ m		
CL	0.5167/6	0.4221/5	0.3573/4
FOSD	0.5097/6	0.4186/5	0.3555/4
HOSD	0.5062/6	0.4168/5	0.3547/4
	$h=0.00635$ m		
CL	2.4836/5	1.8005/4	1.4800/3
FOSD	2.3540/5	1.7532/4	1.4640/3
HOSD	2.3120/5	1.7340/4	1.4537/3
	$h=0.0127$ m		
CL	15.457/5	9.1600/4	6.4280/3
FOSD	12.006/5	7.9080/4	5.9730/3
HOSD	11.288/5	7.5840/4	5.8325/3
FOSD-W/SCF	11.516/5	7.7154/4	5.8938/3

Table 5 Critical torsional load ($N/m \times 10^6$)/wave number (45, 45, −45 deg)$_s$

	$L/R=1$	$L/R=2$	$L/R=5$
	$h=0.001905$ m		
CL	0.4326/9	0.2286/7	0.1077/5
FOSD	0.4239/9	0.2268/7	0.1068/5
HOSD	0.4169/9	0.2259/7	0.1068/5
	$h=0.003175$ m		
CL	1.5255/7	0.7952/6	0.3538/4
FOSD	1.4430/7	0.7759/6	0.3521/4
HOSD	1.4117/7	0.7672/6	0.3503/4
	$h=0.00635$ m		
CL	8.5980/5	4.3963/5	1.9196/3
FOSD	7.0691/6	4.0109/5	1.8811/3
HOSD	6.6382/6	3.8901/5	1.8635/3
	$h=0.0127$ m		
CL	52.547/4	24.500/4	10.17/3
FOSD	29.565/5	18.740/4	9.0820/3
HOSD	26.115/5	17.551/4	8.7750/3
FOSD-W/SCF	27.288/5	18.023/4	8.9064/3

Table 6 Critical torsional load ($N/m \times 10^6$)/wave number (−45, 45, −45 deg)$_s$

	$L/R=1$	$L/R=2$	$L/R=5$
	$h=0.001905$ m		
CL	0.2522/12	0.1366/9	0.0692/6
FOSD	0.2487/12	0.1369/9	0.0692/6
HOSD	0.2469/12	0.1348/9	0.0683/6
	$h=0.003175$ m		
CL	0.8827/10	0.4747/7	0.2251/5
FOSD	0.8512/10	0.4712/7	0.2241/5
HOSD	0.8346/10	0.4641/7	0.2241/5
	$h=0.00635$ m		
CL	4.8079/7	2.5480/6	1.1419/4
FOSD	4.3087/8	2.4520/6	1.1384/4
HOSD	4.0985/8	2.3995/6	1.1244/4
	$h=0.0127$ m		
CL	26.570/5	13.889/5	6.1650/3
FOSD	19.231/6	12.085/5	5.9900/3
HOSD	17.462/6	11.525/5	5.9030/3
FOSD-W/SCF	18.321/6	11.805/5	5.9551/3

radius-to-thickness ratios correspond to a thin cylinder, and for the last two the cylinder is considered to be moderately thick. The length of the shell is also varied to correspond to L/R ratios equal to 1, 2, and 5. Different R/h and L/R ratios are considered to achieve the objective of the present study, that is, to determine the applicability of the different shell theories to the analysis of moderately thick shells.

The following observations can be made from the results in Tables 1-9. For the first two radius-to-thickness ratios $R/h=100$ and 60 (thin cylinders), and for $L/R=1$, the classical theory predicted higher values for the critical torsional load than the other two theories did. As the shells became long, $L/R=5$, the three theories predicted identical results. The maximum difference in critical values observed for $L/R=1$ between classical theory and first-order shear deformation theory is about 2 and 7% for the stacking sequence (45, −45, −45 deg)$_s$, which corresponds to $R/h=100$ and 60, respectively. The maximum difference in critical values observed for $L/R=1$ between classical theory and higher order shear deformation theory is about 3 and 10% for the stacking

Table 7 Critical torsional load ($N/m \times 10^6$)/wave number (45, −45, −45 deg)$_s$

	$L/R=1$	$L/R=2$	$L/R=5$
	$h=0.001905$ m		
CL	0.4134/10	0.2137/8	0.0963/5
FOSD	0.4046/10	0.2119/8	0.0963/5
HOSD	0.4011/10	0.2102/8	0.0955/5
	$h=0.003175$ m		
CL	1.4844/9	0.7531/7	0.3293/4
FOSD	1.3836/9	0.7316/7	0.3284/4
HOSD	1.3521/9	0.7225/7	0.3275/4
	$h=0.00635$ m		
CL	8.1795/6	4.2211/5	1.7865/4
FOSD	6.8833/6	3.9580/5	1.7165/4
HOSD	6.6206/6	3.8795/5	1.6989/4
	$h=0.0127$ m		
CL	46.782/4	23.440/4	9.0900/3
FOSD	27.516/5	18.040/5	8.3370/3
HOSD	25.178/5	16.920/5	8.1620/3
FOSD-W/SCF	25.729/5	17.217/5	8.2233/3

Table 8 Critical torsional load ($N/m \times 10^6$)/wave number (−45, −45, 45 deg)$_s$

	$L/R=1$	$L/R=2$	$L/R=5$
	$h=0.001905$ m		
CL	0.1419/14	0.0854/10	0.0497/7
FOSD	0.1410/14	0:.0854/10	0.0487/7
HOSD	0.1401/14	0.0853/10	0.0497/7
	$h=0.003175$ m		
CL	0.4799/12	0.2819/9	0.1576/6
FOSD	0.4729/12	0.2802/9	0.1576/6
HOSD	0.4659/12	0.2802/9	0.1576/6
	$h=0.00635$ m		
CL	2.5080/9	1.4677/7	0.7602/5
FOSD	2.3785/9	1.4360/8	0.7602/5
HOSD	2.2804/9	1.4187/8	0.7584/5
	$h=0.0127$ m		
CL	13.486/7	7.6020/6	3.7306/4
FOSD	11.244/7	7.0060/6	3.6782/4
HOSD	10.851/7	6.8571/6	3.6340/4
FOSD-W/SCF	10.921/7	5.8500/6	3.6519/4

Table 9 Critical torsional load ($N/m \times 10^6$)/wave number (30, 30, −60 deg)$_s$

	$L/R=1$	$L/R=2$	$L/R=5$
	$h=0.001905$ m		
CL	0.3030/9	0.1384/7	0.0613/5
FOSD	0.2978/9	0.1375/7	0.0613/5
HOSD	0.2934/9	0.1366/7	0.0613/5
	$h=0.003175$ m		
CL	1.1875/8	0.4992/6	0.2084/4
FOSD	1.1087/8	0.4887/6	0.2067/4
HOSD	1.0719/8	0.4834/6	0.2067/4
	$h=0.00635$ m		
CL	7.9518/6	2.9775/5	1.1489/3
FOSD	6.1478/6	2.7320/6	1.1279/3
HOSD	5.6923/7	2.6450/5	1.1157/3
	$h=0.0127$ m		
CL	56.048/5	18.640/4	6.1920/3
FOSD	27.218/6	14.222/4	5.6398/3
HOSD	23.855/6	13.240/4	5.4820/3
FOSD-W/SCF	24.889/6	13.662/4	5.5610/3

sequence (30, 30, -60 deg)$_s$, which corresponds to $R/h = 100$ and 60, respectively. For the thickest shell considered ($R/h = 15$), the maximum difference in the critical values between classical theory and first-order shear deformation theory is about 51% for the stacking sequence (30, 30, -60 deg)$_s$. This corresponds to $L/R = 1$, and the maximum difference in the critical values for the shear deformation theories is about 12% for the same stacking sequence, which, again, corresponds to $L/R = 1$. Regardless of stacking sequence and total thickness, the critical load decreases with increasing L/R ratio. Clearly, the decrease in the critical load is stacking sequence dependent. A final observation is that the number of full waves corresponding to the buckling mode decreases as the ratio L/R and the thickness h increases.

In the first-order shear deformation theory, the transverse shear strains are assumed to be constant through the thickness, which contradicts the conditions of zero shear stresses on the top and the bottom surface of the shell. This requires a shear correction to the transverse shear stiffnesses. Results are presented for the thickest shell considered ($R/h = 15$), for the case of first-order theory with a shear correction factor equal to the value 5/6. It is clearly shown that these results lie between those corresponding to FOSD without a shear correction factor and those corresponding to HOSD, but lie closer to the HOSD results. The maximum difference in the critical values observed for $L/R = 1$ between FOSD-W/SCF and HOSD is a little less than 5% for the stacking sequence (-45, 45, -45 deg)$_s$.

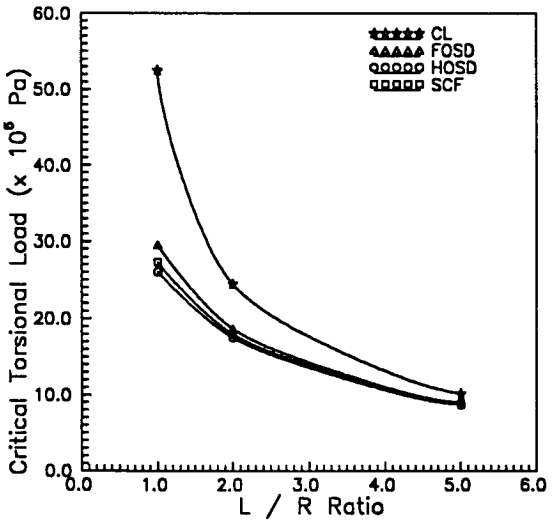

Fig. 2 Critical torsional load for (45, 45, -45 deg)$_s$, $R/h = 15$.

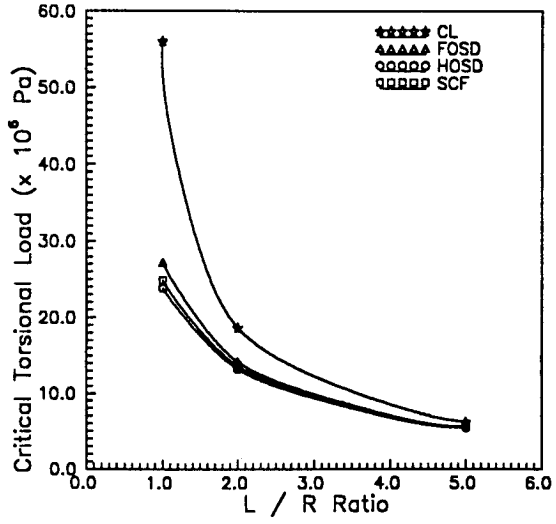

Fig. 3 Critical torsional load for (30, 30, -60 deg)$_s$, $R/h = 15$.

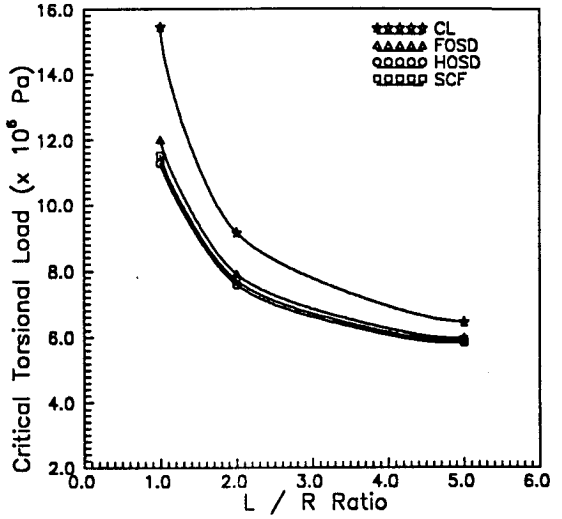

Fig. 4 Critical torsional load for (90, 90, 0 deg)$_s$, $R/h = 15$.

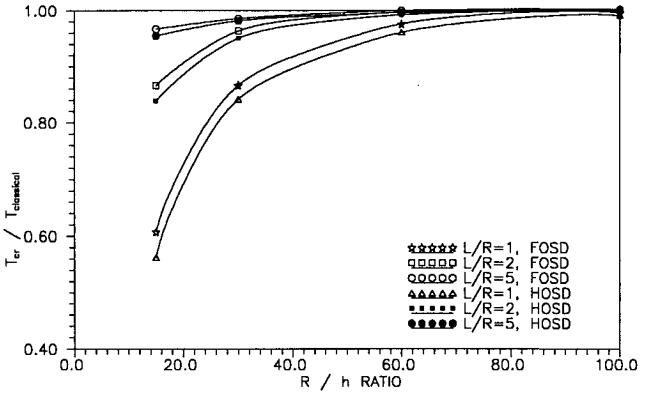

Fig. 5 Normalized critical torsional load for (0, 90, 0 deg)$_s$.

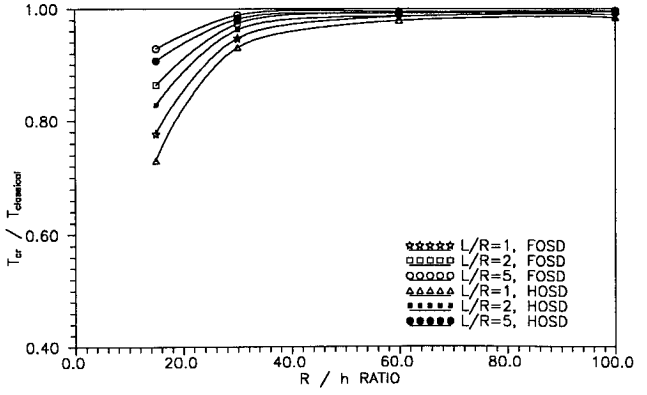

Fig. 6 Normalized critical torsional load for (90, 90, 0 deg)$_s$.

The generated results are represented graphically (Figs. 2–4) for some of the stacking sequences and $R/h = 15$ only. In all figures it is clearly shown that the difference among the three theories is large for small L/R ratios and the difference decreases as the ratio L/R increases, which indicates that the effect of shear deformations is more dominant in short cylinders than it is in long cylinders. Figures 5–9 show the ratio of the critical values predicted by the two shear deformation theories to the values predicted by the classical theory for some of the stacking sequences, as well as those for all L/R and R/h ratios. It is shown that the difference between the different theories diminishes as the R/h ratio and L/R ratio increase.

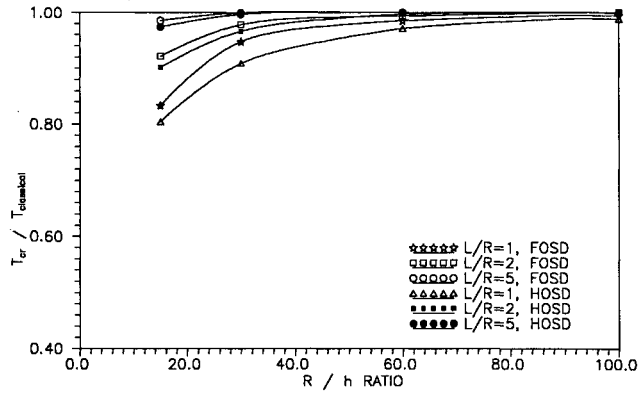

Fig. 7 Normalized critical torsional load for $(-45, -45, 45\ \text{deg})_s$.

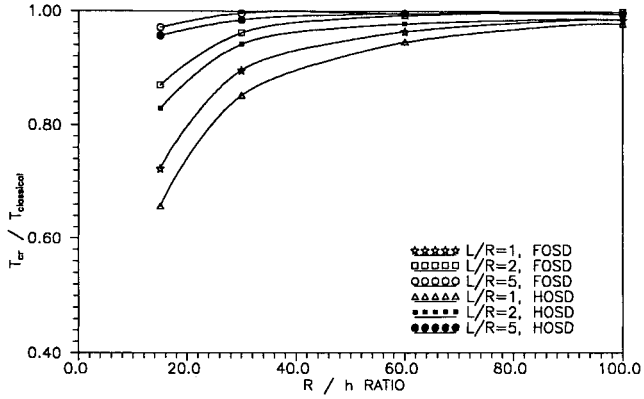

Fig. 8 Normlized critical torsional load for $(-45, 45, -45\ \text{deg})_s$.

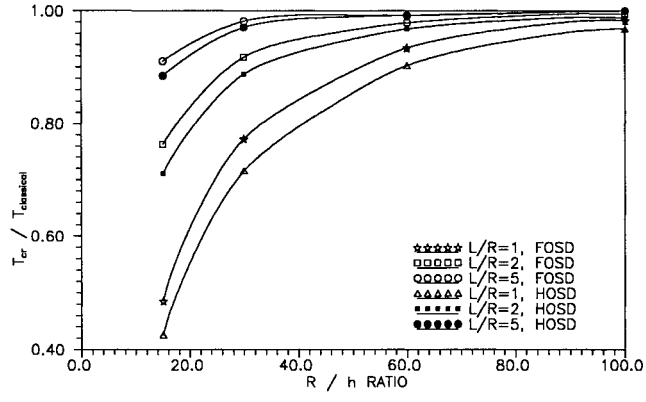

Fig. 9 Normalized critical torsional load for $(30, 30, -60\ \text{deg})_s$.

In summary, classical theory predicted higher values for critical loads than the first-order shear deformation theory, and the last theory predicted higher values for the critical loads than the higher order shear deforamation theory. For thin cylinders ($R/h > 30$), classical theory and shear deformation theories predicted almost identical results. Thus, for thin cylinders classical theory is applicable, and there is no need for higher order shear deformation theories which lead to a lengthy and cumbersome procedure. For moderately thick cylinders ($R/h < 30$), classical theory predicted much higher loads and therefore is not applicable. The greatest difference observed between classical and first-order theory, for $R/h = 15$, is 51%. On the other hand, the greatest difference observed between first-order and higher order theory is 12%, which makes first-order shear deformation theory a good candidate for the analysis of moderately thick cylindrical shells of finite length. Moreover, using a shear correction factor of 5/6 reduces the difference between the two shear deformation theories and predicts critical loads close to the ones predicted by the higher order shear deformation theory (which is known to predict values of critical loads close to those obtained by three-dimensional analyses, see Ref. 5). Finally, it is observed that the strongest configuration in resisting positive shear loads (largest buckling loads) for $R/h = 15$ and all R/L values corresponds to $(45, 45, -45\ \text{deg})_s$. The weakest corresponds to $(-45, -45, 45\ \text{deg})_s$, whereas the configuration $(45, -45, -45\ \text{deg})_s$ is close second to $(45, 45, -45\ \text{deg})_s$. If the direction of the shear load were reversed, the strong and weak configurations would change places.

Appendix: Buckling Integrated Stress Strain Relations

The small additional integrated stresses are related to the kinematics by:

$$N_{xx} = A_{11}\epsilon^o_{xx} + T_{12}K^{-1}_{\theta\theta} + A_{12}\epsilon^o_{\theta\theta} + D_{12}K^2_{\theta\theta} + T_{16}K^{-1}_{x\theta} + A_{16}\gamma_{x\theta} + D_{16}K^{-1}_{x\theta}$$

$$N_{\theta\theta} = A_{12}\epsilon^o_{xx} + T_{22}K^{-1}_{\theta\theta} + A_{22}\epsilon^o_{\theta\theta} + D_{22}K^2_{\theta\theta} + T_{26}K^{-1}_{x\theta} + A_{26}\gamma_{x\theta} + D_{26}K^{-1}_{x\theta}$$

$$N_{x\theta} = A_{16}\epsilon^o_{xx} + T_{26}K^{-1}_{\theta\theta} + A_{26}\epsilon^o_{\theta\theta} + D_{26}K^2_{\theta\theta} + T_{66}K^{-1}_{x\theta} + A_{66}\gamma_{x\theta} + D_{66}K^{-1}_{x\theta}$$

$$N_{\theta z} = T_{44}K^{-1}_{\theta z} + A_{44}\gamma^o_{\theta z} + D_{44}K^2_{\theta z} + A_{45}\gamma^o_{xz} + D_{45}K^2_{xz}$$

$$N_{xz} = T_{45}K^{-1}_{\theta z} + A_{45}\gamma^o_{\theta z} + D_{45}K^2_{\theta z} + A_{55}\gamma^o_{xz} + D_{55}K^2_{xz}$$

$$M_{xx} = D_{11}K^1_{xx} + F_{11}K^3_{xx} + AA_{12}K^{-1}_{\theta\theta} + D_{12}K^1_{\theta\theta} + AA_{16}K^{-1}_{x\theta} + D_{16}K^1_{x\theta} + F_{16}K^3_{x\theta}$$

$$M_{\theta\theta} = D_{12}K^1_{xx} + F_{12}K^3_{xx} + AA_{22}K^{-1}_{\theta\theta} + D_{22}K^1_{\theta\theta} + AA_{26}K^{-1}_{x\theta} + D_{26}K^1_{x\theta} + F_{26}K^3_{x\theta}$$

$$M_{x\theta} = D_{16}K^1_{xx} + F_{16}K^3_{xx} + AA_{26}K^{-1}_{\theta\theta} + D_{26}K^1_{\theta\theta} + AA_{26}K^{-1}_{x\theta} + D_{26}K^1_{x\theta} + F_{26}K^3_{x\theta}$$

$$M_{\theta z} = AA_{44}K^{-1}_{\theta z} + D_{44}K^1_{\theta z}$$

$$M_{xz} = AA_{45}K^{-1}_{\theta z} + D_{45}K^1_{\theta z}$$

$$K_{xx} = D_{11}\epsilon^o_{xx} + BB_{12}K^{-1}_{\theta\theta} + D_{12}\epsilon^o_{\theta\theta} + F_{12}K^2_{\theta\theta} + BB_{12}K^{-1}_{x\theta} + D_{16}\gamma^o_{x\theta} + F_{16}K^2_{x\theta}$$

$$K_{\theta\theta} = D_{12}\epsilon^o_{xx} + BB_{22}K^{-1}_{\theta\theta} + D_{22}\epsilon^o_{\theta\theta} + F_{22}K^2_{\theta\theta} + BB_{26}K^{-1}_{x\theta} + D_{26}\gamma^o_{x\theta} + F_{26}K^2_{x\theta}$$

$$K_{x\theta} = D_{16}\epsilon^o_{xx} + BB_{26}K^{-1}_{\theta\theta} + D_{26}\epsilon^o_{\theta\theta} + F_{26}K^2_{\theta\theta} + BB_{66}K^{-1}_{x\theta} + D_{66}\gamma^o_{x\theta} + F_{66}K^2_{x\theta}$$

$$K_{\theta z} = BB_{44}K^{-1}_{\theta z} + D_{44}\gamma^o_{\theta z} + F_{44}K^2_{\theta z} + D_{45}\gamma^o_{xz} + F_{45}K^2_{xz}$$

$$K_{xz} = BB_{45}K^{-1}_{\theta z} + D_{45}\gamma^o_{\theta z} + F_{45}K^2_{\theta z} + D_{55}\gamma^o_{xz} + F_{55}K^2_{xz}$$

$$L_{xx} = F_{11}K^1_{xx} + I_{11}K^3_{xx} + DD_{12}K^{-1}_{\theta\theta} + F_{12}K^1_{\theta\theta} + DD_{16}K^{-1}_{x\theta} + F_{16}K^1_{x\theta} + I_{16}K^3_{x\theta}$$

$$L_{\theta\theta} = F_{12}K^1_{xx} + I_{12}K^3_{xx} + DD_{22}K^{-1}_{\theta\theta} + F_{22}K^1_{\theta\theta} + DD_{26}K^{-1}_{x\theta} + F_{26}K^1_{x\theta} + I_{26}K^3_{x\theta}$$

$$L_{x\theta} = F_{16}K_{xx}^{1} + I_{16}K_{xx}^{3} + DD_{26}K_{\theta\theta}^{-1} + F_{26}K_{\theta\theta}^{1} + DD_{26}K_{x\theta}^{-1} + F_{66}K_{x\theta}^{1} + I_{66}K_{x\theta}^{3}$$

$$L_{\theta z} = DD_{44}K_{\theta z}^{-1} + F_{44}K_{\theta z}^{1}$$

$$L_{xz} = DD_{45}K_{\theta z}^{-1} + F_{45}K_{\theta z}^{1}$$

$$\tilde{Q}_{xx} = F_{11}\epsilon_{xx}^{o} + EE_{12}K_{\theta\theta}^{-1} + F_{12}\epsilon_{\theta\theta}^{o} + I_{12}K_{\theta\theta}^{2} + EE_{16}K_{x\theta}^{-1} + F_{16}\gamma_{x\theta}^{o} + I_{16}K_{x\theta}^{2}$$

$$\tilde{Q}_{x\theta} = F_{16}\epsilon_{xx}^{o} + EE_{26}K_{\theta\theta}^{-1} + F_{26}\epsilon_{\theta\theta}^{o} + I_{26}K_{\theta\theta}^{2} + EE_{66}K_{x\theta}^{-1} + F_{66}\gamma_{x\theta}^{o} + I_{66}K_{x\theta}^{2}$$

$$P_{\theta\theta} = T_{12}\epsilon_{xx}^{o} + AA_{12}K_{xx}^{1} + DD_{12}K_{xx}^{3} + R_{22}K_{\theta\theta}^{-1} + T_{22}\epsilon_{\theta\theta}^{o} + AA_{22}K_{\theta\theta}^{1} + BB_{22}K_{\theta\theta}^{2} + R_{26}K_{x\theta}^{-1} + T_{26}\gamma_{x\theta}^{o} + AA_{26}K_{x\theta}^{1} + BB_{26}K_{x\theta}^{2} + DD_{26}K_{x\theta}^{3}$$

Next the shell stiffness parameters are defined.

$$A_{ij}, D_{ij}, F_{ij}, I_{ij} = \int_{-h/2}^{h/2} \bar{Q}_{ij}(1, z^2, z^4, z^6)\, dz$$

$$AA_{ij}, BB_{ij}, DD_{ij}, EE_{ij} = \int_{-h/2}^{h/2} \bar{Q}_{ij}(R+z)^{-1}(z, z^2, z^3, z^4)\, dz$$

$$T_{ij} = \int_{-h/2}^{h/2} \bar{Q}_{ij}(R+z)^{-1}\, dz$$

$$R_{ij} = \int_{-h/2}^{h/2} \bar{Q}_{ij}(R+z)^{-2}\, dz$$

References

[1]Reddy, J. N., *Energy and Variational Methods in Applied Mechanics,* Wiley, New York, 1984, pp. 64–122.

[2]Reddy, J. N., "A Review of Refined Theories of Laminated Composite Plates," *Shock and Vibration Digest,* Vol. 22, Jan. 1990, pp. 3–17.

[3]Noor, A. K., and Burton, W. S., "Assessment of Shear Deformation Theories for Multilayered Composite Plates," *Applied Mechanics Reviews,* Vol. 42, No. 1, 1989, pp. 1–13.

[4]Noor, A. K., and Burton, W. S., "Assessment of Computational Models for Multilayered Composite Shells," *Applied Mechanics Reviews,* Vol. 43, No. 4, 1990, pp. 67–97.

[5]Khdeir, A., Reddy, J., and Frederick, D., "A Study of Bending, Vibration and Buckling of Cross-Ply Circular Cylindrical Shells with Various Shell Theories," *International Journal of Engineering Science,* Vol. 27, No. 11, 1989, pp. 1337–1351.

[6]Simitses, G. J., and Anastasiadis, J., "Buckling of Axially-Loaded, Moderately-Thick, Cylindrical Laminated Shells," *Composites Engineering,* Vol. 1, No. 6, 1991, pp. 375–391.

[7]Simitses, G. J., and Anastasiadis, J., "Shear Deformable Theories for Cylindrical Laminates—Equilibrium and Buckling with Applications," *AIAA Journal,* Vol. 30, No. 3, 1992, pp. 826–834.

[8]Simitses, G. J., "Buckling of Eccentrically Stiffened Cylinders Under Torsion," *AIAA Journal,* Vol. 6, No. 10, 1968, pp. 1856–1860.

[9]Simitses, G. J., "Instability of Orthotropic Cylindrical Shells Under Combined Torsion and Hydrostatic Pressure," *AIAA Journal,* Vol. 5, No. 8, 1967, pp. 1463–1469.

[10]Simitses, G. J., and Han, B., "Analysis of Laminated Cylindrical Shells Subject to Torsion," *Developments in Theoretical and Applied Mechanics,* Vol. XVI, Univ. of Tennessee Space Inst., Tullahoma, TN, 1992, pp. II.15.25–II.15.35.

[11]Stein, M., "Nonlinear Theory for Plates and Shells Including the Effects of Transverse Shearing," *AIAA Journal,* Vol. 24, No. 9, 1986, pp. 1537–1544.

[12]Simitses, G. J., *Elastic Stability Of Structures,* Prentice-Hall, Englewood Cliffs, NJ, 1976, Chaps. 6 and 7; also 2nd printing, R. E. Krieger, Melbourne, FL, 1985.

[13]Yamaki, N., *Elastic Stability of Circular Cylindrical Shells,* North-Holland, Amsterdam, The Netherlands, 1984, pp. 45–65.

[14]Jones, R., *Mechanics of Composite Materials,* McGraw-Hill, New York, 1975, Chaps. 4–6.